Chinese Chemical Letters 34 (2023) 108038

Contents lists available at ScienceDirect

Chinese Chemical Letters

journal homepage: www.elsevier.com/locate/cclet

Chiral selection of Tröger's base-based macrocycles with different ethylene glycol chains length in crystallization

Haohui Feng[a,1], Yuan Chen[a,1], Ranran Wang[a], Pengbo Niu[a], Conghao Shi[a], Zhen Yang[a], Ming Cheng[a,c,*], Juli Jiang[a,b,*], Leyong Wang[a]

[a] Jiangsu Key Laboratory of Advanced Organic Materials, School of Chemistry and Chemical Engineering, Nanjing University, Nanjing 210023, China
[b] Maanshan High-Tech Research Institute of Nanjing University, Maanshan 238200, China
[c] The Cancer Hospital of the University of Chinese Academy of Sciences (Zhejiang Cancer Hospital), Institute of Basic Medicine and Cancer (IBMC), Chinese Academy of Sciences, Hangzhou 310022, China

ARTICLE INFO

Article history:
Received 17 September 2022
Revised 27 November 2022
Accepted 1 December 2022
Available online 5 December 2022

Keywords:
Supramolecular macrocycle
Tröger's base
Chiral selection
Rectangular cavity
Glycol chains

ABSTRACT

In the present work, two Tröger's base-based macrocycles (TBBMs) with different bridging ethylene glycol chains (**T1**, n = 1; **T3**, n = 3) were successfully synthesized and studied *via* the crystal analysis. These two TBBMs possess rare rectangular-like cavities and show chiral selection during the crystallization. **T1** with short glycol chain (n = 1) crystallized as racemates, while **T3** with long glycol chain (n = 3) was found as meso isomer. In contrast to **T1** and **T3**, for **T2** (n = 2) both rac-**T2** and meso isomer $R_{2N}S_{2N}$-**T2** has been observed in our previous report. Thus, the synthesis of new TBBMs **T1** and **T3** with different bridging ethylene glycol chains not only makes the study of TBBMs more systematically, but also helps to understand the relationship between the size of the rectangular cavity and the chiral selection of Tröger's base-based macrocycles during their crystallization.

Macrocycles have always been considered as an important component and a key point since the establishment of supramolecular chemistry [1–8]. Through their interaction with guest molecules, well-organized supramolecular assemblies could be created, which have attracted great interest in various research fields especially for materials and biomedical science [9–15]. Among the macrocycle family, chiral macrocycles exhibit a wide range of applications including enantioselective recognition, chiral switching, chirality sensing, chiral catalysis, circularly polarized luminescence and biomedical applications [16–21]. Therefore, chiral macrocycles' synthesis may open new paths for the development of supramolecular chemistry in the future.

Tröger's base unit is a chiral building block with a V-shaped heterocyclic structure, which was first synthesized and reported by J. Tröger in 1887 [22], and confirmed by M. A. Spielman in 1935 [23]. Since then, Tröger's base unit has caught the attention of chemists due to their special V-shaped structure and inherent chirality. Based on Tröger's base unit, many interesting functional systems have been constructed and applied in various fields [24–31]. Recently, in our previous report, we have reported a Tröger's base-based macrocycle TBBM **T2** constructed by two Tröger's base heterocycle (Scheme 1b) [32,33]. Herein, we report two new chiral macrocycles TBBM **T1** and **T3** with different bridging ethylene glycol chain lengths and different chiral selection behaviors during their crystallization (Scheme 1a). The crystal structure comparison revealed that these three TBBMs **T1**, **T2** and **T3** bridging with different ethylene glycol chains exhibited different chiral selectivity behavior during their crystallization. For **T1**, bridging with a shorter mono-ethylene glycol chains, a pair of enantiomeric isomers R_{4N}-**T1** and S_{4N}-**T1** were formed. Different from **T1**, for **T2** bridging with a bit longer di-ethylene glycol chains, both a pair of enantiomeric isomers (R_{4N}-**T2** and S_{4N}-**T2**) and a meso isomer ($R_{2N}S_{2N}$-**T2**) were formed. Whereas, for **T3** bridging with a much longer tri-ethylene glycol chains, only a meso isomer $R_{2N}S_{2N}$-**T3** was produced. These results indicate that Tröger's base units exhibited chiral selection during the crystallization of TBBMs. The synthesis of TBBMs **T1** and **T3** not only makes the study of TBBMs more systematical, but also helps to understand the relationship between the size of the rectangular cavity and the chiral selection of Tröger's base-based macrocycles during the crystallization of TBBMs.

As shown in Scheme 2, the target Tröger's base-based macrocycles TBBM **T1**, **T2** and **T3** were synthesized starting from

* Corresponding authors.
E-mail addresses: ming.cheng2015@foxmail.com (M. Cheng), jjl@nju.edu.cn (J. Jiang).
[1] These authors contributed equally to this work.

https://doi.org/10.1016/j.cclet.2022.108038
1001-8417/

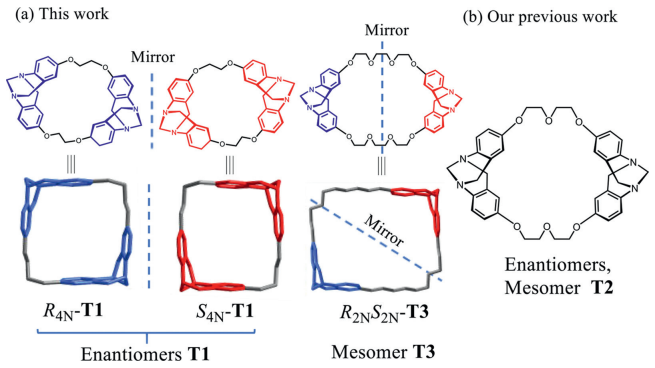

Scheme 1. (a) Stereo-isomer structures observed in crystal analyses of TBBMs **T1** and **T3**. (b) TBBM **T2** previously reported by us.

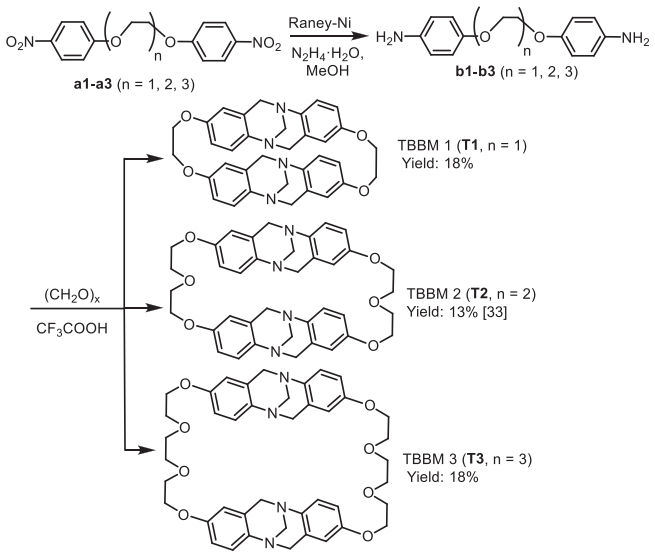

Scheme 2. Synthetic route of TBBMs **T1**, **T2** and **T3**.

glycol-bridged nitroaromatic compounds [33,34]. Firstly, the glycol-bridged *p*-nitrobenzene compound **a1-a3** was reduced to the corresponding amine **b1-b3**. Then, the engendered amine group was reacted with formaldehyde in the presence of trifluoroacetic acid to form Tröger's base units. Through this synthetic route, **T1**, **T2** and **T3** were successfully synthesized in the yields of 18%, 13% and 18% respectively (Section 2.1-2.2 in Supporting information for more details). The structures of **T1** and **T3** were characterized by ^{1}H NMR, ^{13}C NMR, and high-resolution electrospray ionization mass spectroscopy (HR-ESI-MS). In the ^{1}H NMR spectrum (Figs. S2 and S6 in Supporting information), the characteristic peaks at chemical shifts (δ 4.49 ppm for **T1**, 4.60 ppm for **T3**) are observed which can be explained by the Tröger's base skeleton. In the HR-ESI-MS of **T1** and**T3** (Figs. S5 and S9 in Supporting information), peaks were found at *m/z* 561.2480 and 737.3543 assigned to $[\mathbf{T1}+\mathrm{H}]^+$ (calcd. 561.2496) and $[\mathbf{T3}+\mathrm{H}]^+$ (calcd. 737.3545), respectively.

After the successful synthesis of **T1** and **T3**, we tried to grow single crystals of **T1** and **T3** in order to confirm the sizes of their cavities. Luckily, the single crystals of **T1** and **T3** suitable for X-ray crystallography were obtained by slow diffusion of isopropyl ether into trichloromethane and dichloromethane solution of **T1** and **T3**. Similar to **T2**, due to the V-skeleton of Tröger's base, the single crystal structure analysis showed that both **T1** and **T3** presented structure with an approximately rectangular cavities. Theoretically, due to the inherent chirality of Tröger's base skeleton, TBBMs with two Tröger's base units should have one pair enantiomeric isomers and one meso isomer at the same time. However, by comparing chirality of **T1**, **T2** and **T3** in the crystal structure, different chiral selection phenomena were observed in the crystal structures. As shown in Fig. 1, for **T1** bridging with a shorter mono-ethylene glycol chains (n = 1), only a pair of enantiomers R_{4N}-**T1** and S_{4N}-**T1** were observed in the crystal structure. Unlike **T1**, for **T2** bridged with a bit longer di-ethylene glycol chains (n = 2), both a pair of enantiomeric isomers R_{4N}-**T2** and S_{4N}-**T2** and a meso isomer ($R_{2N}S_{2N}$-**T2**) were observed in the crystal structure which is completely consistent with the theoretical derivation. However, differently to both **T1** and **T2**, for **T3** bridging with a much longer tri-ethylene glycol chains (n = 3), only the meso isomer $R_{2N}S_{2N}$-**T3** was found in the crystal structure. Thus, based on these finding, the crystallisation experiments showed that the reactions are diastereoselective in the case of **T1** and **T3**, and non-diastereoselective in the case of **T2**. Moreover, the length of the bridging chains have a significant impact on the chiral behavior of Tröger's base-based macrocyclic molecules during their crystallization.

According to single crystal analysis, for TBBM **T1**, the cavity size defined as the maximum diagonal length distance between two bridging methylene carbons was 11.7 Å, and the average dimensions was 8.1×8.7 Å^2. For **T2**, bridged with a bit longer di-ethylene glycol chains, the cavity size of *rac*-**T2** was 14.2 Å in maximum diagonal length, and the average dimensions was 11.2×8.2 Å^2, which is a slightly larger than that of **T1** (Fig. 1). The cavity size of $R_{2N}S_{2N}$-**T3** was 16.8 Å in maximum diagonal with average dimensions of 13.0×10.7 Å^2, which is barely bigger than *meso* isomer $R_{2N}S_{2N}$-**T2** with average dimensions of 10.9×8.8 Å^2. These data indicate that the cavity size of macrocyclic molecules increases significantly with the lengthening of the ethylene glycol chain. In addition, the crystal structures show that, for all TBBMs **T1**, **T2** and **T3**, the ethylene glycol units at the bridging corners

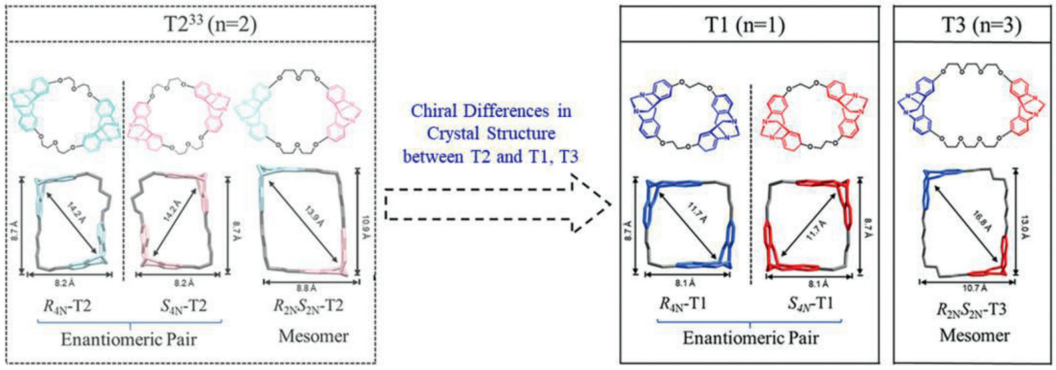

Fig. 1. Crystal structure of *rac*-**T1**, *rac*-**T2**, *meso*-**T2** and *meso*-**T3**. Tröger's base units with S_NS_N were drawn in red, while Tröger's base units with R_NR_N were drawn in blue.

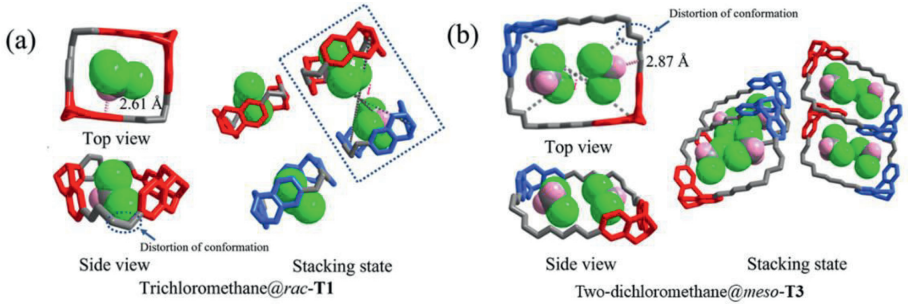

Fig. 2. Single crystal of complex (a) trichloromethane@**T1**, (b) two-dichloromethane@**T3**. Corresponding molecule structural formulas: C, gray; H, pink; O, red; Cl, green. *i*: inversion center.

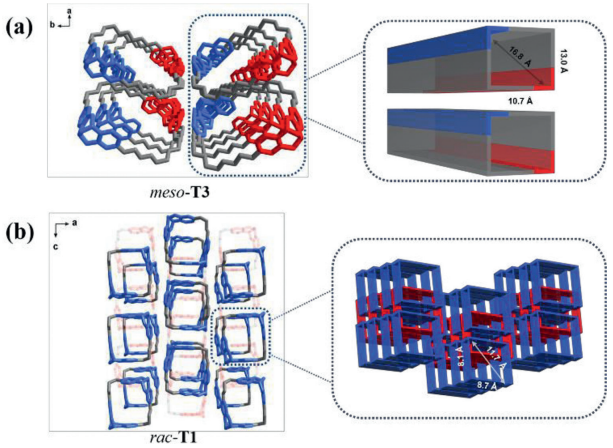

Fig. 3. (a) *meso*-**T3** was stacked along the *c*-axis as a channel. (b) *rac*-**T1** was stacked as a channel across layer along the *b*-axis.

exist in the highest energy *cis*-conformation rather than in the lowest energy *trans*-conformation, indicating that there are higher tensions in the TBBMs **T1**, **T2** and **T3**. Due to this high tension during the synthesis process, the precursors of TBBMs do not easily form cyclic molecules, resulting in their lower synthetic yields.

Furthermore, **T1**, and **T3** exhibited different abilities in encapsulating solvent molecules. As shown in Fig. 2, *rac*-**T1** can form 1:1 host-guest complex trichloromethane@**T1**, in which obvious one hydrogen bond between the hydrogen atom of trichloromethane and the oxygen atom on **T1** could be observed. In contrast, *meso*-**T3** can simultaneously combine two dichloromethane molecules to form a 1:2 host-guest complex two-dichloromethane@**T3**, four hydrogen bonds between chlorine atom of dichloromethane and the hydrogen atom of **T3** could be observed. The other interesting phenomenon is that in the crystal packing structure of trichloromethane@*rac*-**T1**, if chloroform@*rac*-**T1** is considered as a whole, an inversion center could be found in the crystal structure. Similarly, the same phenomenon was achieved for two-dichloromethane@*meso*-**T3**. These results suggest that the packing behavior of macrocyclic molecules in crystals also follows chirality rules. Moreover, there are some other interesting findings in the crystal. According to our previous reports, **T2** was found to form long-range channels in the crystal packing structure. As shown in Fig. 3a, for **T3**, the long-range ordered channels could also be found although **T3** and **T2** have different chiral behaviors. But for *rac*-**T1**, when considering both R_{4N}-**T1** and S_{4N}-**T1**, **T1** does not stack into a channel in the crystal packing structure, however when only R_{4N}-**T1** or S_{4N}-**T1** with a single chirality is considered, the crystal packing structure of **T1** has obvious long-range channel packing (Fig. 3b).

In conclusion, we synthesized two novel Tröger's based macrocycles TBBMs **T1** and **T3** with different ethylene glycol chain lengths. Although starting materials are very similar, the TBBMs **T1** and **T3** exhibit different chiral behavior during crystallization. Combined with **T2** reported by us before, an obvious chiral selection during the crystallization process of TBBMs could be found. For **T1**, bridging with a shorter mono-ethylene glycol chains, a pair of enantiomeric isomers R_{4N}-**T1** and S_{4N}-**T1** were formed in the crystal structure. Different from **T1**, for **T2** bridged with a bit longer di-ethylene glycol chains, both a pair of enantiomeric isomers (R_{4N}-**T2** and S_{4N}-**T2**) and a meso isomer ($R_{2N}S_{2N}$-**T2**) were formed in the crystal structure. For **T3** bridging with a much longer tri-ethylene glycol chains, only meso isomer $R_{2N}S_{2N}$-**T3** was observed in the crystal structure. The length of the bridge chain (n = 1, 2, 3) affects the chiral selectivity during TBBM crystal formation, which provide new methods for the chiral synthesis and purification of macrocycles with high tension. The synthesis of two TBBMs **T1** and **T3** made the research of TBBMs more systematically, which is also helpful to understand the relationship between the size of the rectangular cavity and the chiral selection of Tröger's base-based macrocycles during the cyclization of TBBMs. We believe that our research may provide new references for the chiral synthesis and purification of chiral macrocycles. Based on this research, our ongoing research work are mainly focused on: (1) Looking for guest molecules (including chiral guest molecules) that have strong binding abilities to Tröger's base-based macrocycles. (2) Hydrophilic modification of Tröger's base-based macrocycles and study their recognition properties and applications in water. (3) Exploring their potential applications in chiral catalysis.

Declaration of competing interest

The authors declare that they have no known competing financial interests or personal relationships that could have appeared to influence the work reported in this paper.

Acknowledgments

We gratefully acknowledge the financial support from the National Natural Science Foundation of China (Nos. 21901113, 21871135) and the Natural Science Foundation of Jiangsu Province (No. BK20190287). This research work was also financially supported by the Starry Night Science Foundation of Zhejiang University Shanghai Institute for Advanced Study (No. SN-ZJU-SIAS-006). We also thank Dr. Khouloud Djebbi for her kind help with language modification.

Supplementary materials

Supplementary material associated with this article can be found, in the online version, at doi:10.1016/j.cclet.2022.108038.

References

[1] Y. Wang, H. Wu, J.F. Stoddart, Acc. Chem. Res. 54 (2021) 2027–2039.
[2] L. Yang, X. Wang, H. Yao, W. Jiang, Acc. Chem. Res. 53 (2020) 198–208.
[3] R. Peng, Y. Xu, Q. Cao, Chin. Chem. Lett. 29 (2018) 1465–1474.
[4] Z. Liu, S.K.M. Nalluri, J.F. Stoddart, Chem. Soc. Rev. 46 (2017) 2459–2478.
[5] T. Ogoshi, T. Yamagishi, Y. Nakamoto, Chem. Rev. 16 (2016) 7937–8002.
[6] Y. Wang, H. Wu, J.F. Stoddart, Acc. Chem. Res. 54 (2021) 2027–2039.
[7] K. Xu, Z.Y. Zhang, Z. Zhou, C. Li, Chin. Chem. Lett. 33 (2022) 2451–2454.
[8] Z.Y. Zhang, C. Li, Acc. Chem. Res. 55 (2022) 916–929.
[9] S. Li, Y. Gao, Y. Ding, A. Xu, H. Tan, Chin. Chem. Lett. 32 (2021) 313–318.
[10] G.R. Desiraju, Nature 412 (2001) 397–400.
[11] T. Xiao, J. Wang, Y. Shen, et al., Chin. Chem. Lett. 32 (2021) 1377–1380.
[12] D. Qu, Q. Wang, Q. Zhang, X. Ma, H. Tian, Chem. Rev. 115 (2015) 7543–7588.
[13] J. Yang, D. Dai, L. Ma, Y. Yang, Chin. Chem. Lett. 32 (2021) 729–734.
[14] T. Guo, A. Li, J. Xu, K.K. Baldridge, J. Siegel, Angew. Chem. Int. Ed. 60 (2021) 25809–25814.
[15] D.A. Poole, S. Mathew, J.N.H. Reek, J. Am. Chem. Soc. 143 (2021) 16419–16427.
[16] X. Han, P. Li, Y. Han, C. Chen, Angew. Chem. Int. Ed. 61 (2022) e202202527.
[17] S. Tong, J. Li, D. Liang, et al., J. Am. Chem. Soc. 142 (2020) 14432–14436.
[18] H. Zhu, Qi Li, B. Shi, et al., J. Am. Chem. Soc. 142 (2020) 17340–17345.
[19] Y. Chen, S. Pangannaya, B. Sun, et al., ACS Appl. Bio Mater. 4 (2021) 2066–2072.
[20] Y. Ma, M. Quan, X. Lin, et al., CCS Chem. 2 (2020) 1078–1092.
[21] C. Shi, H. Li, X. Shi, L. Zhao, H. Qiu, Chin. Chem. Lett. 33 (2022) 3613–3622.
[22] J. Tröger, J. Prakt. Chem. 36 (1887) 225–245.
[23] M.A. Spielman, J. Am. Chem. Soc. 37 (1935) 583–585.
[24] Q. Yang, Y.Y. Cai, Z.Y. Zhu, et al., ACS Appl. Mater. Interfaces 12 (2020) 24806–24816.
[25] Y. Zhao, K. Chen, E.A. Yildiz, et al., Chem. Eur. J. 26 (2020) 3591–3599.
[26] C. Zhang, R. Huang, H. Tang, et al., J. Membr. Sci. 597 (2020) 117763.
[27] H. Hong, Z. Guo, D. Yan, H. Zhan, Microporous Mesoporous Mater. 294 (2020) 109870.
[28] S. Dawaigher, K. Månsson, E. Ascic, et al., J. Org. Chem. 80 (2015) 12006–12014.
[29] A. Jarzebski, G. Schnakenburg, A. Lützen, ChemPlusChem 85 (2020) 1455–1464.
[30] S. Shanmugaraju, C. Dabadie, K. Byrne, Chem. Sci. 8 (2017) 1535–1546.
[31] S. Shanmugaraju, D. Umadevi, L.M. González-Barcia, Chem. Commun. 55 (2019) 12140–12143.
[32] Y. Chen, C. Qian, Q. Zhao, et al., Chem. Commun. 55 (2019) 8072–8075.
[33] Y. Chen, M. Cheng, B. Hong, et al., Front. Chem. 7 (2019) 383.
[34] A.A. Ibrahim, M. Matsumoto, Y. Miyahara, et al., J. Heterocycl. Chem. 35 (1998) 209–215.